

PAPER

Fast Single Image De-Hazing Using Characteristics of RGB Channel of Foggy Image

Dubok PARK[†], David K. HAN^{††}, Changwon JEON[†], *Nonmembers*, and Hanseok KO^{†a)}, *Member*

SUMMARY Images captured under foggy conditions often exhibit poor contrast and color. This is primarily due to the air-light which degrades image quality exponentially with fog depth between the scene and the camera. In this paper, we restore fog-degraded images by first estimating depth using the physical model characterizing the RGB channels in a single monocular image. The fog effects are then removed by subtracting the estimated irradiance, which is empirically related to the scene depth information obtained, from the total irradiance received by the sensor. Effective restoration of color and contrast of images taken under foggy conditions are demonstrated. In the experiments, we validate the effectiveness of our method compared with conventional method.

key words: *air-light, de-hazing, depth estimation, image restoration*

1. Introduction

Images of objects in fog in general exhibit poor contrast and corrupted colors. One source of the degradation is that the light from the object is attenuated as it travels through the fog, resulting less image radiance reaching the imaging sensor. Ambient light scattered by fog particles, called “air-light” [1]–[4], creates a significant source of degradation as it gets added to the image, resulting poor contrast. The former effect can be viewed as reduction in signal strength while the latter phenomenon adds noise to the weakened signal.

Recently, a vehicle borne black-box system with a video camera is receiving interests in auto industry for its potential utility of analyzing and reconstructing auto accidents. However, under foggy condition, the system may not yield images with sufficient clarity for post-accident analyses.

It has been demonstrated, however, that foggy images can be restored by physics-based methods with scene depth (e.g., d) information [4]–[8]. From a monocular image, however, estimating scene depth from the corresponding 2-dimensional image is not trivial. Saxena et al. proposed an algorithm which estimates scene depth from monocular images [9].

They used a Markov Random Field (MRF) for incorporating multi-scale features with a relational depth model to estimate scene depth. However, the method requires

complex computation related to extracting depth information from image features at multiple scales.

Recently, there have been a number of studies aimed at the restoration of monocular fog-degraded images. Tan et al. proposed a fog-degraded image enhancement method using color constancy [10]. They used a color invariant property under foggy conditions. However, this method could not successfully eliminate the actual air-light because scene depth estimation was not employed. K. He et al. restored a foggy image using the dark channel prior for estimating the transmission map [11]. However, this method requires large computation, thereby taking up a significant processing time.

In this paper, we propose a physics-based method of restoration that can be applied to foggy images by means of scene depth estimation. Essentially, the proposed method estimates scene depth using relative changes of RGB components of light as it propagates through fog.

This paper is organized as follows. In Sect. 2, we describe the atmospheric scattering model that represents the scene radiance and air-light irradiance. Section 3 describes the proposed scene depth estimation algorithm. In Sect. 4, we show how the scene radiance is restored. In Sect. 5, we present the experimental results and validate the effectiveness of our method. Finally, we present our concluding remarks in Sect. 6.

2. Atmospheric Scattering Model

Scattering of light by propagation media is the main reason of image degradation in foggy scenes. Therefore, to remove the fog effect in degraded images, it is necessary to analyze scattering mechanisms of light. In general, the exact nature of scattering is highly complex and depends on the types, orientation, size and distributions of particles constituting the media as well as wavelengths, polarization states and direction of the incident light [12].

Narasimhan et al. summarized the aforementioned degradation process of ‘Attenuation’ and ‘Air-light’ [13]. The attenuation of object radiance decreases exponentially as its depth from the observer increases. The second factor causes the atmosphere to behave like a source of light, and is thus referred to as air-light. Ambient light scattered by particles in the atmosphere causes this phenomenon. Based on these two factors, the total irradiance received by the sensor is usually described by the sum of the direct attenuated irradiance and the air-light irradiance as depicted in Fig. 1.

Manuscript received April 17, 2012.

Manuscript revised January 17, 2013.

[†]The authors are with the School of Electrical Engineering, Korea University, Seoul, Korea.

^{††}The author is with the Office of Naval Research, Arlington, VA, USA.

a) E-mail: hsko@korea.ac.kr

DOI: 10.1587/transinf.E96.D.1793

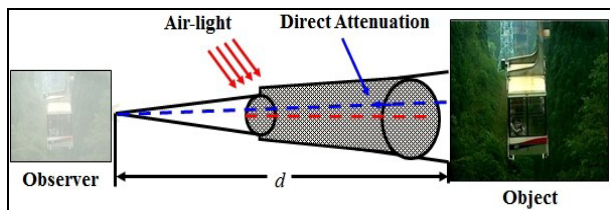


Fig. 1 Atmospheric scattering model.

Equation (1) is the atmospheric scattering model which is widely used in foggy images [11], [14].

$$\mathbf{I}(\mathbf{x}) = \mathbf{J}(\mathbf{x})e^{-\beta d(\mathbf{x})} + \mathbf{A}(1 - e^{-\beta d(\mathbf{x})}) \quad (1)$$

where, \mathbf{x} is the spatial location in the image, \mathbf{I} is the observed intensity in the hazy image, \mathbf{J} is the scene radiance, \mathbf{A} is the atmospheric light, which is assumed to be globally constant. d is the depth of the scene point. β is called the scattering coefficient of the atmosphere related to fog density. Again it is assumed to be constant in foggy image. $\mathbf{J}(\mathbf{x})e^{-\beta d(\mathbf{x})}$ is the direct attenuation term and $\mathbf{A}(1 - e^{-\beta d(\mathbf{x})})$ is the air-light term. As the scene depth, d , increases, the air-light accumulates and becomes more intense in the hazy images. Note that, while the other parameters in the equation are scalar, \mathbf{I} , \mathbf{J} , \mathbf{A} are color vectors with RGB components.

If three parameters, β , d , \mathbf{A} , are known, it is possible to calculate \mathbf{J} which represents the true intensity in a clear day.

3. Estimating the Parameters

3.1 Estimating the Scene Depth

As the scene depth increases, the air-light accumulates and becomes more intense in foggy images as in Eq. (1). Figure 2 shows intensities of RGB channels measured on a couple of color test panels under different fog densities.

It is a well-known phenomenon whereby increase of the fog density diminishes the differences of intensities among RGB components. Our method extracts depth information by exploiting the relationship between the propagation depth and the RGB component equalization.

We define the Euclidean norm of $\mathbf{Z}(\mathbf{x})$ to measure the degree of differences between the RGB channels.

$$\|\mathbf{Z}(\mathbf{x})\|_2 = \left(\sum_{i=1}^3 |z_i(\mathbf{x})|^2 \right)^{1/2} \quad (2)$$

in which

$$z_1(\mathbf{x}) = R(\mathbf{x}) - G(\mathbf{x}) \quad (3)$$

$$z_2(\mathbf{x}) = G(\mathbf{x}) - B(\mathbf{x}) \quad (4)$$

$$z_3(\mathbf{x}) = B(\mathbf{x}) - R(\mathbf{x}) \quad (5)$$

where, R , G , B denote the intensity of each RGB channels respectively and \mathbf{x} is the spatial location in an image.

Figure 3 shows the relationship between $\mathbf{Z}(\mathbf{x})$ and the fog density which consists of 100 levels of fog densities.

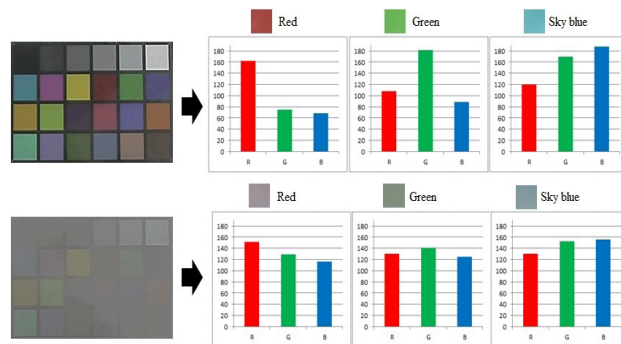


Fig. 2 Intensity of each RGB channel at different fog density.

$\mathbf{Z}(\mathbf{x})$ decreases as the fog density increases except for grey scale (black and white) as shown in Fig. 3. However, it is noted that the 3 major color channels (R, G, B) are very responsive to various levels of fog densities.

From Fig. 3, it can be inferred that $\mathbf{Z}(\mathbf{x})$ decreases as the scene depth increases in foggy images. Figure 4 shows the relationship between $\mathbf{Z}(\mathbf{x})$ and relative scene depth in field images. Relative scene depth is determined manually for comparison. From the calculated norm of $\mathbf{Z}(\mathbf{x})$, the scene depth can be estimated for each pixel. However, computing $\mathbf{Z}(\mathbf{x})$ for each pixel can make different depth region even though pixels are in the same depth region. To avoid this problem, we estimate the scene depth by combing a group of pixels by a patch. We propose the scene depth estimation of a patch of pixels by:

$$d(\mathbf{x}) = 1 - \alpha \cdot \max_{\mathbf{y} \in \Omega(\mathbf{x})} \|\mathbf{Z}(\mathbf{y})\|_2 \quad (6)$$

Here, α is a normalizing parameter to ensure the range of $d(\mathbf{x})$ remains from 0 to 1. \mathbf{x} is the spatial location in an image and $\Omega(\mathbf{x})$ is a local patch centered at \mathbf{x} . From experiments, we found a local patch size of 30×30 computationally expedient with sufficient level of accuracy in the depth estimates for reasonable images. However, since the depth obtained from Eq. (6) is estimated for local patch, block artifacts may occur as shown in Fig. 5 (b). To prevent the block artifact, we refine the scene depth using a guided filter [15].

The guided filter performs as an edge-preserving smoothing operator like the bilateral filter [16], but it delivers better performance near the edges. The process of refining scene depth using the guided filter is a linear transformation using coefficients of a_k , b_k defined by:

$$a_k = \frac{\frac{1}{|w|} \sum_{i \in w_k} I_i d_i - \mu_k \bar{d}_k}{\sigma_k^2 + \varepsilon}, \quad \forall i \in w_k \quad (7)$$

$$b_k = \bar{d}_k - a_k \mu_k \quad (8)$$

where $|w|$ is the number of pixels in w_k , I is a gray-scale hazy image, and d is estimated depth from Eq. (6). w_k is a window centered at the k -th pixel. μ_k and σ_k^2 are the mean and variance of I in w_k . \bar{d}_k is the mean of d in w_k . ε is a regularization parameter preventing a_k from becoming too large. ε is set to 10^{-4} in the experiment. Refined depth using

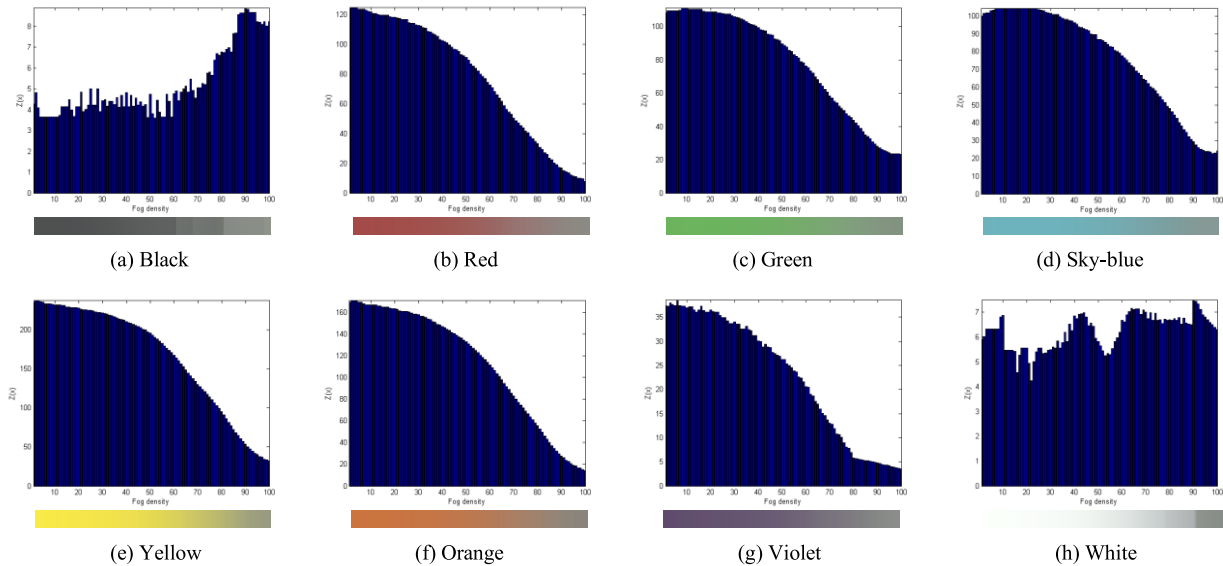


Fig. 3 Relationship with $Z(x)$ and fog density in various colors.



Fig. 4 Relationship between $Z(x)$ and Relative scene depth: (a) Foggy image, (b) Relative scene depth, (c) Results of $Z(x)$.

the coefficients (a_k, b_k) is obtained by

$$\tilde{d}_i = \bar{a}_i I_i + \bar{b}_i \tag{9}$$

in which

$$\bar{a}_i = \frac{1}{|w_i|} \sum_{k \in w_i} a_k, \quad \bar{b}_i = \frac{1}{|w_i|} \sum_{k \in w_i} b_k \tag{10}$$

Figure 5 shows the scene depth estimating procedure. Figure 5 (c) is refined scene depth using Eq. (9). Figure 5 (d) is a relative scene depth made by manually to compare estimated scene depth qualitatively.

3.2 Estimating the Atmospheric Light

Atmospheric light exists in most haze-opaque regions. In the previous work, A is used as the sky brightness [4] or as the largest intensity in the image [10]. However, the atmospheric light chosen only by intensity or brightness is not always the most haze-opaque region. In this paper, we search the atmospheric light as follows. We first pick the top 5% of the highest pixels of refined depth experimentally as a trade-off between the accuracy and the reliability. More specifically, as the percentage becomes smaller, the atmospheric lights can be estimated more accurately, but the estimated information is less reliable since a smaller number of pixels are employed. Among these pixels, the one with the highest intensity is selected as the atmospheric light.

3.3 Estimating the Scattering Coefficient

The scattering coefficient is the degree of fog density. As fog density increases, scattering coefficient is also increased.

Generally, a dense foggy image has a small standard deviation because most of the intensity is concentrated near the air-light term.

The variance of pixel values of the gray-scaled fog image can be expressed as

$$I(\mathbf{x}) = J(\mathbf{x})e^{-\beta d(\mathbf{x})} + A(1 - e^{-\beta d(\mathbf{x})}) \tag{11}$$

$$\begin{aligned} \sigma_I^2 &= \frac{1}{N} \sum_{i=1}^N \left(I(i) - \frac{1}{N} \sum_{j=1}^N I(j) \right)^2 \\ &= e^{-2\beta d} \frac{1}{N} \sum_{i=1}^N \left(J(i) - \frac{1}{N} \sum_{j=1}^N J(j) \right)^2 \end{aligned} \tag{12}$$

where, Eq. (11) is the gray-scaled fog image and N represents the number of pixels in the image. We postulate that

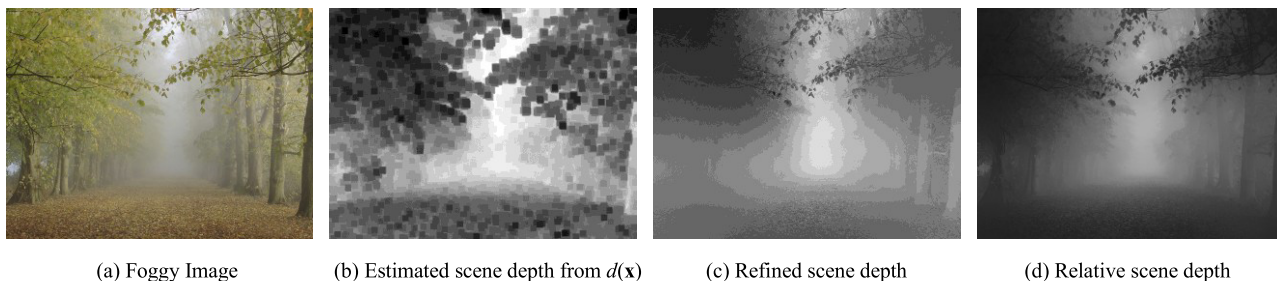


Fig. 5 Proposed method of the scene depth estimating procedure.

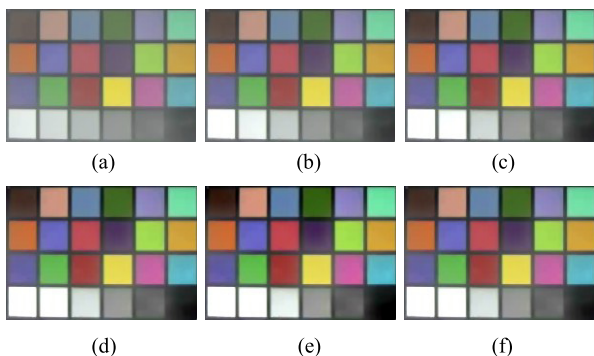


Fig. 6 Recovered images under different scattering coefficient values: (a) Foggy image, (b) Recovered image ($\beta = 0.4$), (c) Recovered image ($\beta = 0.6$), (d) Recovered image ($\beta = 0.8$), (e) Recovered image ($\beta = 1$) (f) Recovered image by proposed method ($\beta = 0.7822$).

scene depth, d , is what is needed to show the relationship with variance and the scattering coefficient.

The variance of the scene radiance, $J(\mathbf{x})$, which has zero scattering coefficient ($\beta = 0$) is expressed as

$$\sigma_o^2 = \frac{1}{N} \sum_{i=1}^N \left(J(i) - \frac{1}{N} \sum_{j=1}^N J(j) \right)^2 \quad (13)$$

From Eqs. (12) and (13), σ_I^2 is expressed as

$$\sigma_I^2 = e^{-2\beta} \sigma_o^2 \quad (14)$$

From Eq. (14), the scattering coefficient can be expressed as

$$\beta = \ln \sigma_o - \ln \sigma_I \quad (15)$$

Since the σ is changed at each image, Eq. (15) can be expressed using the first order Taylor Series approximation at one

$$\beta = 1 + \ln \sigma_o - \sigma_I \quad (16)$$

Generally, the variance of the scene radiance approximates one. Therefore, Eq. (16) can be changed as

$$\beta = 1 - \sigma_I \quad (17)$$

Therefore, we can estimate the scattering coefficient by incorporating the standard deviation of dense foggy image from Eq. (17).

As can be seen by this expression, the dense foggy image should have large scattering coefficient, since the standard deviation of the input image is small. Figure 6 shows the recovered images using scattering coefficient acquired from Eq. (17) and under different scattering coefficient values.

4. Restoring the Scene Radiance

With the scene depth and the scattering coefficient, we can restore the scene radiance using Eq. (1). The scene radiance $\mathbf{J}(\mathbf{x})$ is restored by:

$$\mathbf{J}(\mathbf{x}) = \mathbf{A} - (\mathbf{A} - \mathbf{I}(\mathbf{x}))e^{\beta d(\mathbf{x})} \quad (18)$$

The restored images generally look dim because the scene radiance was attenuated as the light propagates through the fog. Examples of restored images are shown in Fig. 7.

5. Experimental Results

We implemented the proposed algorithm using MATLAB 2011b and desktop computer with a 2.67 GHz i7 processor. We compared our method with Tan's work [10] and He's work [11]. In Fig. 7, the proposed method restored foggy regions in the input images and reconstructed fine details of the input images. From Fig. 8 to Fig. 10, we compared our method with that of Tan's [10] and He's work [11]. In Fig. 8 and Fig. 9, some fog regions are not removed effectively in Tan's work, because maximizing the contrast tends to over-estimate the haze layer. Tan's approach over-saturated and over-stretched the contrast in Fig. 10. He's approach shows good results from Fig. 8 to Fig. 10. Our method restores foggy image retaining color fidelity and removes haze.

We compared computational requirement of the proposed method to the other methods. As the image size is increased, processing time of the conventional approach increased exponentially as shown in Table 1. For large images such as 3456×2304 , He's approach could not be processed due to a large memory requirement. Our method took about 132.5 sec to process the same image as shown in Table 1. We also compared performance of the proposed method with other conventional methods in terms of Global Contrast Factor (GCF) [17] measure to show the image quality quantitatively. GCF is an evaluation indicator capturing the degree of contrast quality. As the contrast in the image is increased,



Fig. 7 De-hazing procedure from foggy image: (a) Foggy images (b) Estimated scene depth from $d(x)$ (c) Refined scene depth images using guided filter (d) De-hazing results of our approach.

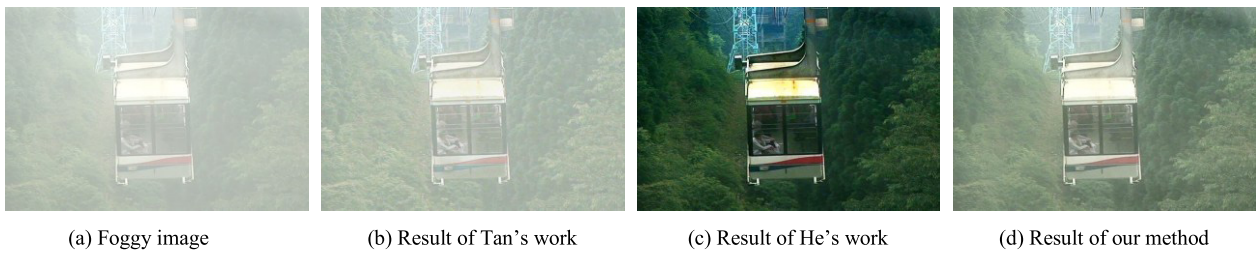


Fig. 8 Comparison of experimental result with conventional works (image size 720×480).

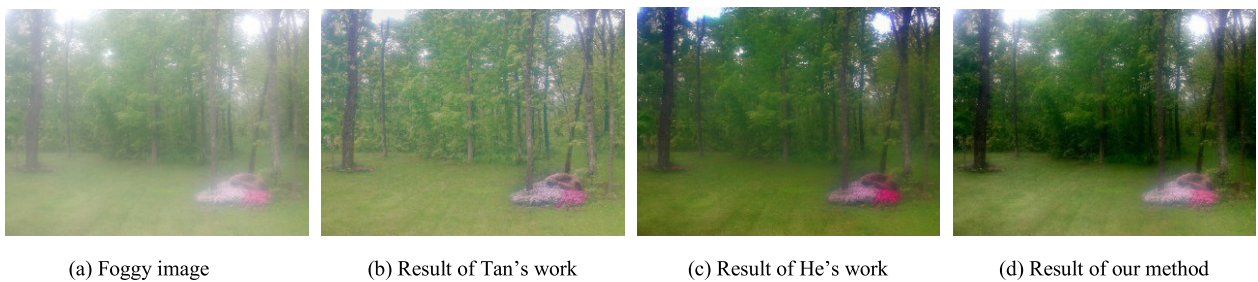


Fig. 9 Comparison of experimental result with conventional works (image size 800×600).

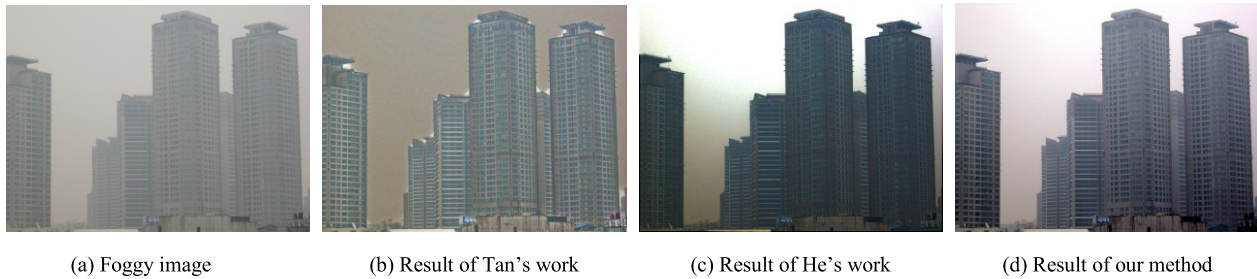


Fig. 10 Comparison of experimental result with conventional works (image size 1600×1200).

Table 1 Processing time comparison with conventional works.

Image size	Tan's work	He's work	Proposed
640 x 480	13.4 sec	60.8 sec	5.2 sec
720 x 480	18.8 sec	67.7 sec	6.3 sec
800 x 600	35.8 sec	96.1 sec	8.1 sec
1600 x 1200	483.2 sec	4785.6 sec	31.6 sec
3456 x 2304	9783.4 sec	Impossible	132.5 sec

Table 2 Evaluation indicator score (GCF).

	Fig. 8	Fig. 9	Fig. 10
Foggy Image	1.364172	2.296338	0.938296
Tan's work	2.142925	4.932664	2.871196
He's work	3.616716	3.487145	2.051730
Proposed	2.893867	4.468292	2.070932

the GCF value becomes high. Table 2 shows the GCF score of experimental results from Fig. 8 to Fig. 10.

Although arguably conventional methods yielded better image quality as shown in Table 2, it requires a large amount of computation and memory to restore image effectively. Clearly, He's method may be impractical for restoring large images or movie files. Our proposed method demonstrated its performance in restoring foggy images at reasonable quality with low computational cost. Further, it may be most suitable for restoring movies with foggy images for its computational efficiency.

6. Conclusions

In this work, we proposed a foggy image de-hazing algorithm using a physical model and characteristics of RGB channels from single monocular image. The proposed method first estimates the scene depth using Euclidean norm of each RGB channel differences. Then, the proposed method estimates the atmospheric light using the refined scene depth and intensity. Finally, the proposed method estimates the scattering coefficient using the standard deviation of normalized input image. With estimated parameters, the proposed method restores foggy image. From the limited set of experiments, it successfully enhances image qualities retaining color fidelity and processing time.

In conclusion, when applied to practical systems such as a video based surveillance, the proposed algorithm is expected to successfully restore degraded contrast and color of images caused by air-light.

Acknowledgments

This research was supported by Seoul R&BD Program (WR080951).

References

- [1] J.P. Oakley and B.L. Satherley, "Improving image quality in poor visibility conditions using a physical model for contrast degradation," *IEEE Trans. Image Process.*, vol.7, no.2, pp.167-179, Feb. 1998.
- [2] S.G. Narasimhan and S.K. Nayar, "Contrast restoration of weather degraded images," *IEEE Trans. Pattern Anal. Mach. Intell.*, vol.25, no.6, pp.713-724, June 2003.
- [3] D. Kim, C. Jeon, B. Kang, and H. Ko, "Enhancement of image degraded by fog using cost function based on human visual model," *IEEE International Conference on Multisensor Fusion and Integration for Intelligent Systems (MFI)*, pp.64-67, Aug. 2008.
- [4] S.K. Nayar and S.G. Narasimhan, "Interactive de-weathering of an image using physical models," *Proc. ICCV Workshop on Color and Photometric Methods in Computer Vision*, Oct. 2003.
- [5] Y. Zhu, B. Fang, and H. Zhang, "Image de-weathering for road based on physical model," *International Conference on Information Engineering and Computer Science (ICIECS)*, pp.1-4, Dec. 2009.
- [6] X. Wang and Z. Tang, "Automatic image de-weathering using physical model and maximum entropy," *IEEE Conference on Cybernetics and Intelligent Systems*, pp.996-1001, Sept. 2008.
- [7] L. Hongjun, Z. Yan, and W. Xinwei, "Study of defog technology based on scattering model in assistant driving system," *2nd International Congress on Image and Signal Processing (CISP)*, pp.1-4, Oct. 2009.
- [8] J.-P. Tarel, N. Hautière, A. Cord, D. Gruyer, and H. Halmaoui, "Improved visibility of road scene images under heterogeneous fog," *IEEE Intelligent Vehicles Symposium (IV)*, pp.478-485, June 2010.
- [9] A. Saxena, S. Chung, and A. Ng, "Learning depth from single monocular images," *Neural Information Processing Systems (NIPS)*, vol.18, 2005.
- [10] R. Tan, "Visibility in bad weather from a single image," *IEEE Conference on Computer Vision and Pattern Recognition (CVPR)*, pp.1-8, June 2008.
- [11] K. He, J. Sun, and X. Tang, "Single image haze removal using dark channel prior," *IEEE Trans. Pattern Anal. Mach. Intell.*, vol.33, no.12, pp.2341-2353, Dec. 2011.
- [12] Y.Y. Schechner, S.G. Narasimhan, and S.K. Nayar, "Instant de-hazing of images using polarization," *Proc. 2001 IEEE Computer Society Conference on Computer Vision and Pattern Recognition (CVPR)*, vol.1, pp.325-332, 2001.
- [13] S.K. Nayar and S.G. Narasimhan, "Vision in bad weather," *Proc. Seventh IEEE International Conference on Computer Vision*, vol.2, pp.820-827, Sept. 1999.
- [14] N. Hautière, J-P Tarel, J. Lavenant, and D. Aubert, "Automatic fog

detection and estimation of visibility distance through use of an on-board camera,” *J. Machine Vision and Applications* archive, vol.17, no.1, pp.8–20, March 2006.

- [15] K. He, J. Sun, and X. Tang, “Guided image filtering,” *Proc. 11th European Conference on Computer Vision (ECCV 2010)*, pp.1–14, Sept. 2010.
- [16] C. Tomasi and R. Manduchi, “Bilateral filtering for gray and color images,” *Sixth International Conference on Computer Vision*, pp.839–846, Jan. 1998.
- [17] K. Matkovic, L. Neumann, A. Neumann, T. Psik, and W. Purgathofer, “Global contrast factor —a new approach to image contrast,” *Computational Aesthetics in Graphics, Visualization and Imaging 2005*, pp.159–168, May 2005.



Hanseok Ko (M’95-SM’00) received B.S. degree from Carnegie Mellon University, in 1982, M.S. degree from the Johns Hopkins University, in 1988, and Ph.D. degree from the CUA, in 1992, all in electrical engineering. At the onset of his career, he was with the WOL, Maryland. In March of 1995, he joined the faculty of the Department of Electronics and Computer Engineering at Korea University, where he is currently Professor. His professional interests include signal processing for pattern recognition, multi-modal analysis, and intelligent data fusion.



Dubok Park (M’11) received B.S. degree in Electrical and Computer Engineering from Korea University, Seoul, Korea, in 2010. Since 2010, he has been a Ph.D. student in Korea University. His research interests are in image enhancement and multi-sensor image fusion.



David K. Han received B.S. degree from Carnegie Mellon University, and MSE and PhD from the Johns Hopkins University. After years of serving as scientist at NSWC and ONR, he joined the University of Maryland in College Park in 2005 as a faculty and the deputy director of the CECD. From 2007 to 2009, he was the Distinguished IWS chair professor in the Systems Engineering Department of the United States Naval Academy in Annapolis, MD. In Jan. 2009, Dr. Han returned to ONR as a program officer in the Ocean Engineering team. In summer of 2012, he was appointed as the Deputy Director of Research of ONR.



Changwon Jeon (M’06) received B.S. degree in Electrical and Computer Engineering from Korea University, Seoul, Korea, in 2003. Since 2003, he has been a Ph. D student in Korea University. His research interests are in image enhancement and human-robot interaction.